Electrochemical and Spectroelectrochemical Study of 7,7′-Diapo-(7*E*,7′*Z*)-diphenylcarotene

Dezhong Liu and Lowell D. Kispert*

Department of Chemistry, The University of Alabama, Tuscaloosa, Alabama 35487-0336

Received: June 27, 2000; In Final Form: September 19, 2000

Self-assembled monolayers (SAMs) formed by adsorption of thiols onto gold provide a flexible method to study the electrochemical reactivity of 7,7′-diapo-(7*E*,7′*Z*)-diphenylcarotene **(**DDC) on such barrier monolayers. Barrier properties of three kinds of SAMs (long-chain *n*-alkanethiols, *ω*-substituted alkanethiols, and 4-mercaptopyridine) were investigated. The influence of the *ω*-functional group and the thickness (chain length in *n*-alkanethiols) of the monolayer on the electrochemical reaction of DDC was explored. Electron transfer between solution species and the modified-gold electrode can occur either by tunneling through the monolayer or by approaching the electrode at "pinholes" or defects in the monolayer. Compared to the behavior on bare gold electrodes, the thiol monolayers cause a barrier effect for the reaction of DDC and the adsorption of polymeric products on the Au electrode surface. With increasing chain length of alkanethiol molecules, a stronger barrier effect to the adsorption of polymeric products is observed. DDC and its electrochemical reaction products (including the radical cations and polymers) were also studied by simultaneous optical and electrochemical techniques.

Introduction

A number of studies of self-assembled monolayers (SAMs) have been carried out in the past two decades.[1] Nevertheless, the process of self-assembly and the role of various parameters, which control the formation of a well-ordered, densely packed monolayer at a solid/liquid interface, are not well-understood. In general, the assembly process is thermodynamically driven. SAMs are usually formed on metallic supports (substrates) such as gold, silver, and copper.[2] The constitution of a monolayer surface depends on the molecular structure of SAMs. The functionalized SAMs are used in analysis of affinity and kinetic rate constants.[3] Self-assembly is a versatile technique for surface modification with a number of other applications such as chemical sensors, nonlinear optical materials, and high-density memory devices.[2a] There is a wide variety of substrates along with the monolayers containing different functional groups which are used to form SAMs, but the thiol monolayer on Au has received the most attention due to its simplicity of preparation.[1a]

To date, there has been only one report[4] about the electrochemical behavior of carotenoids on SAM-modified gold electrodes, despite the wide interest concerning applications of SAMs. It is well-known that carotenoids play an active role in photodriven electron transport processes.[5] It is important to determine the structure and properties of carotenoid species which are involved in biochemical, photochemical, and electrochemical processes. 7,7′-Diapo-(7*E*,7′*Z*)-diphenylcarotene (DDC), a synthetic carotenoid, was chosen for study in the present work because of its unique reaction properties on electrode surfaces.[6,7] The cyclic voltammogram (CV) with a platinum (Pt) working electrode is nearly the same as with a bare gold (Au) electrode (Figure 1A, solid line). Polymeric products are formed by reaction of DDC dications with neutral DDC during the electrochemical oxidation process in dichloromethane. Simultaneous electrochemical quartz crystal microbalance measurements[7] showed that the polymeric products have an apparent molar mass of 5400 g per mole of electrons, which corresponds to 11 monomeric units of DDC molecules combined with two electrolyte (TBAHFP) counteranions (PF_6^-). The polymeric products of DD**C** adsorb very strongly on the

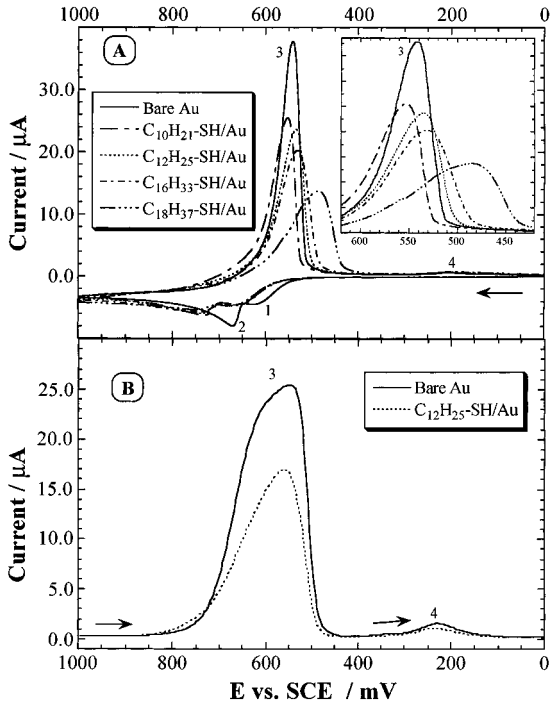

Figure 1. (A) Cyclic voltammograms of 0.9 mM **DDC** in deaerated 0.05 M TBAHFP/CH_2Cl_2 solution using a bare gold electrode, and SAMs-modified gold electrodes containing different chain lengths of alkanethiols. Scan rate 100 mV/s. Insert is the zoom-in of the reduction peak 3 in Figure 1A. (B) Osteryoung square wave voltammograms of 0.9 mM DDC in deaerated 0.05 M TBAHFP/CH_2Cl_2 solution using a bare Au and a DDT-modified gold electrode.

* To whom correspondence should be addressed. Tel: (205)348−8436. Fax: (205)348-9104. E-mail: Lkispert@bama.ua.edu.

10.1021/jp0022860 CCC: $20.00
Published on Web 01/13/2001

SCHEME 1: Electrochemical Reactions of Carotenoids

Heterogeneous electrode reactions:

$$\text{Car} \underset{}{\overset{E^\circ_1}{\rightleftharpoons}} \text{Car}^{\bullet+} + e^- \quad (1)$$

$$\text{Car}^{\bullet+} \overset{E^\circ_2}{\rightleftharpoons} \text{Car}^{2+} + e^- \quad (2)$$

$$^{\#}\text{Car}^{+} + e^- \overset{E^\circ_3}{\rightleftharpoons} {}^{\#}\text{Car}^{\bullet} \quad (3)$$

Homogeneous chemical reactions:

$$\text{Car}^{2+} + \text{Car} \overset{K_{com}}{\rightleftharpoons} 2\,\text{Car}^{\bullet+} \quad (4)$$

$$\text{Car}^{2+} \overset{K_{dp}}{\rightleftharpoons} {}^{\#}\text{Car}^{+} + H^+ \quad (5)$$

$$\text{Car}^{\bullet+} \overset{K'_{dp}}{\rightleftharpoons} {}^{\#}\text{Car}^{\bullet} + H^+ \quad (6)$$

(Note: Car neutral species of the carotenoid
$\text{Car}^{\bullet+}$ radical cation of the carotenoid
Car^{2+} dication of the carotenoid
$^{\#}\text{Car}^{+}$ carotenoid cation with one less proton
$^{\#}\text{Car}^{\bullet}$ carotenoid radical with one less proton)

electrode surface whereas other common carotenoids (such as β-carotene and canthaxanthin) do not show such behavior. It was therefore of particular interest to determine the change in the electrochemical reactivity and adsorption of polymeric products of DDC as a function of SAMs of long chain *n*-alkanethiols and ω-substituted alkanethiols and 4-mercaptopyridine modifying the Au electrodes. The structure of DDC is shown below.

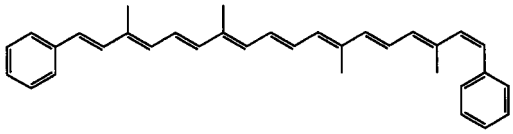

7,7'-Diapo-7*E*,7'*Z*-diphenylcarotene (**DDC**)

The electrochemical reactions of a number of carotenoids in dichloromethane are quasi-reversible or reversible.[8] The results show that, during an electrochemical oxidation−reduction cycle, radical cations, dications, cations (loss of one H^+ from dications), and neutral radicals (loss of one H^+ from radical cations) can be formed. The established electrode and homogeneous reactions are shown[9−11] in Scheme 1.

In the present paper, we report the electrochemical behavior and adsorption of DDC on Au electrodes modified with three kinds of SAMs (long-chain alkanethiols, ω-substituted alkanethiols, and 4-mercaptopyridine), as illustrated in Scheme 2. The primary objective of the present investigation is to understand the barrier effect of SAMs as well as whether different SAMs influence the adsorption of DDC. The monolayers on electrodes will limit the access of solution-phase DDC molecules to the electrode surface. These studies have revealed that SAMs with different chain lengths or terminal groups affect the adsorption and reactivity of DDC in comparison to the bare Au electrodes.

Experimental Section

Chemicals. 7,7′-Diapo-(7*E*,7′*Z*)-diphenylcarotene (DDC) was synthesized as previously described.[12] Tetrabutylammonium hexafluorophosphate (TBAHFP) was purchased from Fluka. Anhydrous dichloromethane (99.8%, CH_2Cl_2) and ethanol (EtOH) were obtained from Aldrich. The following thiols were purchased from Aldrich and used without further purification: 1-octadecanethiol [$CH_3(CH_2)_{17}$−SH, 98%, ODT), 1-hexadecanethiol [$CH_3(CH_2)_{15}$−SH, 92%, HDT], 1-dodecanethiol [$CH_3(CH_2)_{11}$−SH, 98+%, DDT], 1-decanethiol [$CH_3(CH_2)_9$−SH, 98%, 1-DT], 11-mercaptoundecanoic acid [HS−$(CH_2)_{10}$−COOH, 95%, MUA], 11-mercapto-1-undecanol [HS−$(CH_2)_{11}$−OH, 97%, MUO], 4-mercaptopyridine [HS−C_5H_4N, 95%, 4-MP]. Other chemicals were of analytical grade and used as received. All solutions were prepared in a drybox under a nitrogen atmosphere. Except as specifically noted, 0.05 M TBAHFP in CH_2Cl_2 solutions were used as the supporting electrolyte medium in electrochemical measurements.

SCHEME 2: Self-assembled Monolayers on Au Electrodes

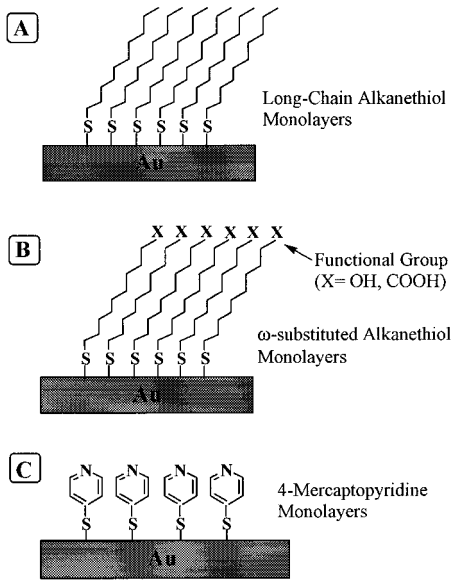

Self-assembly of Thiols on Gold. Polycrystalline gold disk electrodes (2.01 mm^2) were constructed by embedding a piece of a high-purity gold disk (dia. 1.6 mm, 99.99%) in a Teflon plastic rod. The Au electrodes were polished with a soft polishing cloth by using METADI SUPREME polycrystalline diamond suspensions (water base) (BUEHLER) which include 9, 6, 3, and 1 μm diameter particles, starting with the 9 μm diameter particle suspension to polish for 8 min, then 6, 3, and 1 μm particles in sequence. After each size polishing, the disk electrode was washed thoroughly with deionized water and sonicated in deionized water for 3 min. Prior to use, the Au electrodes were dipped for 5 min in a freshly prepared Piranha solution (concentrated H_2SO_4:30%H_2O_2 = 3:1 V/V) (Caution! The Piranha solution reacts violently with organic substances and should be handled with extreme care). The electrodes were rinsed thoroughly with deionized water and then anhydrous ethanol. After being dried in a stream of argon, the gold electrodes were transferred immediately to a 1 mM thiol solution prepared in anhydrous ethanol and then incubated for 24 h in the dark at ambient temperature. The assembly was kept under pure N_2. Just before measurement, the modified Au electrodes were rinsed three times with ethanol and then dried in a gentle stream of high purity argon (99.998%, Post Airgas, Inc.).

Electrochemical Measurement. Cyclic voltammetry and other electrochemical measurements were carried out in a conventional three-electrode system at room temperature with a BAS-100 B/W electrochemical analyzer. For cyclic voltammetry, a bare Au or thiol-modified Au disk electrode was used as the working electrode. A saturated calomel electrode (SCE) and a platinum wire were used as reference and counter electrodes, respectively. A 10 mL cylindrical undivided cell was used for the above measurements. For bulk electrolysis, a platinum gauze electrode was used as the working electrode, and a silver wire was the pseudo reference electrode.

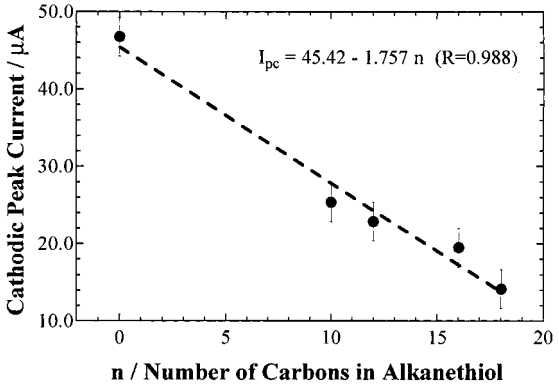

Figure 2. Dependence of cathodic peak current (third peak in CVs) upon the number of carbons in alkanethiols for the SAM-modified Au electrodes.

Simultaneous Electrochemical and Optical Measurements. Optical absorption spectra in the range of 190−1100 nm were recorded with a Shimadzu UV-1601 UV−vis spectrophotometer. A special spectroelectrochemical cell, divided into two chambers by a frit, was used; one chamber was attached to a quartz cuvette (10 mm path length) and used for simultaneous bulk electrolysis and optical measurements.[13,14] A platinum gauze, serving as the working electrode, and a silver wire as pseudo reference were arranged in one chamber to which the quartz cuvette was attached, and a platinum counter electrode was in the other chamber.

Results and Discussion

Cyclic Voltammetry. A typical cyclic voltammetric response of DDC on a bare Au and an alkanethiol-modified Au electrode in 0.05 M TBAHFP/CH_2Cl_2 solution is shown in Figure 1A. In the voltammogram on bare gold, there are two peaks (peaks 1 and 2, their peak potentials are $E_1 = 0.600$ V; $E_2 = 0.675$ V vs SCE) during the anodic scan, which correspond to the two steps of one-electron oxidation of the neutral species and the resulting radical cations of DDC. During the cathodic scan, only one single, greatly enhanced peak 3 (peak potential $E_3 = 0.540$ V vs. SCE for bare gold electrode) and one weak peak 4 (peak potential $E_4 = 0.22$ V), which resulted from the reduction of the transient intermediate $^{\#}Car^{+}$ (reaction 3 in Scheme 1), were observed. The enhanced reduction peak 3 is due to adsorption or electrodeposition of species formed only after the generation of the dications of DDC.[6,7] For the Au electrodes modified with *n*-alkanethiol SAMs (Scheme 2A), the cyclic voltammograms (CVs) and Osteryoung square wave voltammograms (OSWV) depicted in Figure 1 show that the oxidation, reduction, and adsorption features are suppressed to some extent by the monolayers. ODT SAMs provide the largest barrier. The longer the chain length, the larger is the barrier effect. As shown in Figure 2, a good linear relationship between the third peak current in CVs and the number of carbon atoms in the alkanethiol SAMs is obtained. Such barrier properties are evidenced by a decrease of the peak current in OSWV on alkanethiol-modified Au electrodes in comparison to the bare Au electrode (Figure 1B). On the other hand, a large peak-to-peak potential separation occurred with the SAMs modified Au electrode (for ODT/Au electrode, $\Delta E'_1 = E'_1 - E'_3 = 650 - 480 = 170$ mV, at 100 mV/s; compared with the bare Au electrode, $\Delta E_1 = E_1 - E_3 = 600 - 540 = 60$ mV, at 100 mV/s. It is obvious that the monolayers impede electron transfer between the gold electrode and the solution species. It is known from the literature[15,16] that barrier layers on electrodes can suppress background currents, control adsorption, inhibit corrosion, and enable control of electrode processes. Some barrier properties of alkanethiol-modified gold electrodes have been studied,[17] and it was found that SAMs suppress corrosion of Au in acidic Br^- solutions compared to bare Au, and long chain-length alkanethiol-monolayers protect Au better than the shorter SAMs. Our above observations are consistent with the reported results.

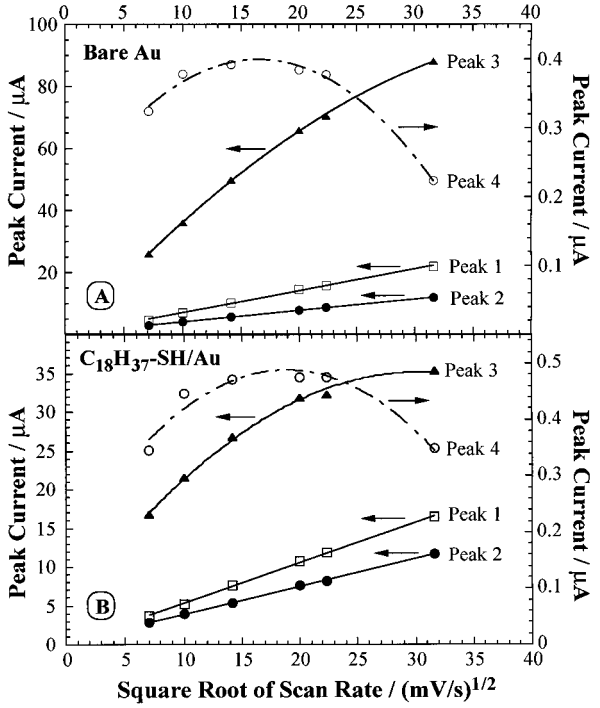

Figure 3. Dependence of peak current on the square root of scan rate in CVs for (A) bare Au and (B) ODT-modified Au electrode. Experimental conditions are same as in Figure 1.

The dependence of four CV peak currents (peaks 1−4) on the square root of the scan rate is shown in Figure 3. Similar phenomena were observed for both bare Au and SAM-modified Au electrodes. The linear behavior observed for the anodic peaks 1 and 2 indicates that they are due to linear diffusion-controlled electron transfer processes. Two other peaks (3 and 4) show a remarkable nonlinear dependence and imply that peak 3 is controlled by adsorption, and peak 4 is kinetically controlled since the peak current has a maximum at a specific scan rate.

Our preliminary work[4] had shown that the rate constant of electron transfer for canthaxanthin is ca. $(1.0 \pm 0.2) \times 10^{-2}$ cm s^{-1} on a bare Au electrode and $(6.0 \pm 2.0) \times 10^{-3}$ cm s^{-1} on an Au electrode modified with ODT. This means that the electron transfer is suppressed to 60% by a long-chain *n*-alkanethiol-modified Au electrode. The above results were deduced by using the DigiSim CV simulation program. For DDC, it is difficult to obtain a precise value of the electron-transfer rate constant because of the complicated mechanism including both electrochemical and adsorption reactions. There is a limitation for the DigiSim program since adsorption cannot be considered in the simulation. On the other hand, we may suppose the same barrier effect (around 40% suppression) for DDC on the ODT-modified Au electrode. Such barrier properties can clearly be seen in Figure 1 by the obvious decrease of cathodic peak intensity. Compared to the bare gold electrode, the alkanethiol monolayers cause a barrier effect for the reaction of DDC and the adsorption of polymeric products on the Au electrode surface. With increasing chain length of alkanethiol

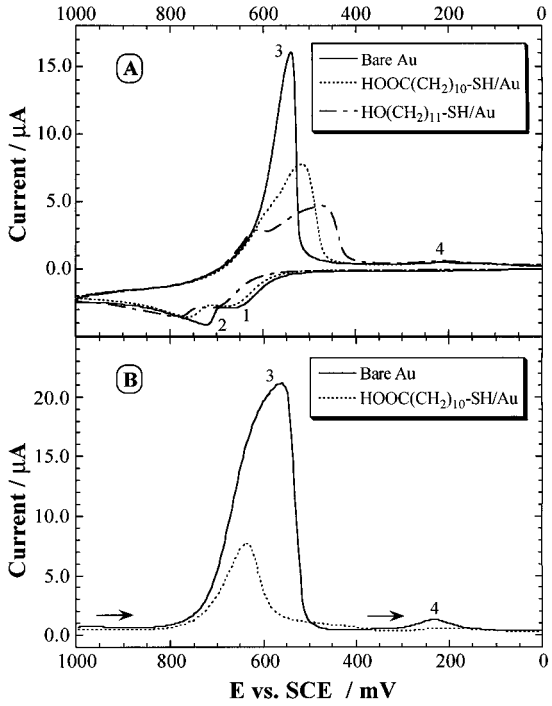

Figure 4. (A) Cyclic voltammograms of 0.9 mM DDC in deaerated 0.05 M TBAHFP/CH_2Cl_2 solution at bare Au, and Au electrodes modified with MUA and MUO. Scan rate 100 mV/s. (B) Osteryoung square wave voltammograms of 0.9 mM DDC in deaerated 0.05 M TBAHFP/CH_2Cl_2 solution using bare Au and MUA-modified Au electrode.

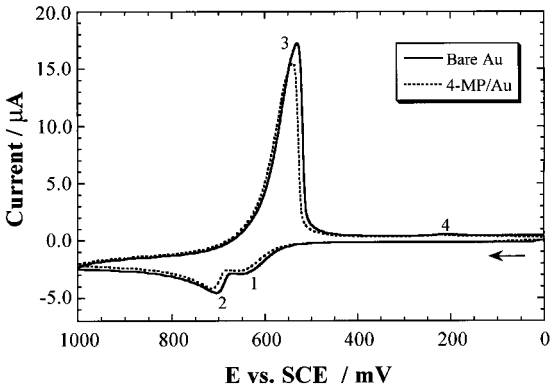

Figure 5. Cyclic voltammograms of 0.9 mM DDC in deaerated 0.05 M TBAHFP/CH_2Cl_2 solution using bare Au and 4-MP-modified Au electrode. Scan rate 100 mV/s.

molecules, a stronger barrier effect to the adsorption of polymeric products is observed.

Figure 4 illustrates the CV and OSWV curves of bare and ω-functionalized thiol-modified electrodes. It is obvious that terminally substituted carboxylic acid and hydroxy SAMs have the same profound barrier effect on the reaction of DDC as *n*-alkanethiol SAMs. In contrast, 4-MP SAMs have only a small barrier effect on the reaction of DDC compared to the bare Au electrode as shown in Figure 5.

The decrease of peak current can be explained in terms of the decrease of electron-transfer (ET) rate and a certain degree of inhibition by the monolayers for the ET to the electrode. That is to say, the reaction of DDC on SAM-modified Au electrodes is partly kinetically limited. For alkanethiol SAMs (including the compounds terminally substituted with a carboxylic acid or a hydroxy group), ET is partially inhibited by the long alkane chain. In contrast, ET proceeds readily through the pyridine rings of 4-MP SAMs. Furthermore, the electrochemical reactions of DDC can still occur even in the presence of long chain alkanethiol SAMs, and this phenomenon correlates with the presence of "pinholes" or defects in the monolayers. This means that electron transfer between solution species and the modified gold electrode can occur either by tunneling through the monolayer or by approaching the electrode at those "pinholes" or defects in the monolayers.

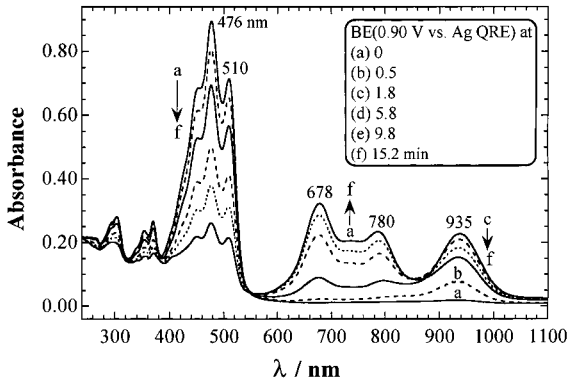

Figure 6. Change in UV−visible absorption spectra for 0.01 mM DDC in a 0.05 M TBAHFP/CH_2Cl_2 solution under bulk electrolysis at different time periods. A potential of 0.90 V vs Ag was applied.

In most cases, the SAMs on electrode surfaces are not perfect. SAMs prepared from long-chain alkanethiols still contain numerous defects.[16,18,19] These defects are formed by imperfect deposition of SAMs on the Au electrode surface or subsequent partial desorption of the modified molecules from the Au surface during potential cycling in dichloromethane medium. Our contact angle gonimetric measurements of long-chain alkanethiol SAM-modified Au electrodes gave the high contact angle values of water (90°−98°), which indicates that the SAMs are densely packed on the Au electrode surface. Therefore, the possibility of defects is mainly related to the stability and durability of the SAMs in the reaction medium, especially in organic solvents. Experimental results showed that the reduction peak current increased about 10% after 10 successive potential cycling (at the rate of 100 mV/s) in dichloromethane medium. This change is attributed to the creation of pinholes in the monolayers on the electrode surface. The defects in the monolayers behave as an ultramicroelectrode ensemble.[16,18a] Defects in the SAMs permit partial or complete penetration of DDC molecules into the Au electrode surface. Hence, the ET rate between DDC and the Au electrode will vary widely near defect structures. Kinetic heterogeneity is expected for SAM-modified Au electrodes.

Optical and Simultaneous Spectroelectrochemical Studies. To understand more about the properties of DDC and its electrochemical reaction products, simultaneous spectroelectrochemical experiments were performed by using bulk platinum working electrodes. The molar extinction coefficient of DDC in 0.05 M TBAHFP/CH_2Cl_2 was estimated to be 8.0 (±0.2) × 10^4 (λ_{max} = 476 nm) which is comparable to the literature data of the following carotenoids in different solvents: β-carotene, 1.3 × 10^5 (λ_{max} = 465 nm, in $CHCl_3$); canthaxanthin, 1.2 × 10^5 (λ_{max} = 480 nm, in benzene); 10′-apo-β-caroten-10′-al, 8.2 × 10^4 [λ_{max} = 435 nm, in light petroleum (bp 40−60 °C)].[20]

Bulk electrolysis (using a platinum gauze electrode as working electrode) and simultaneous optical absorption measurements in the range of 240−1100 nm were carried in 0.05 M TBAHFP/CH_2Cl_2 in order to identify the reaction product of DDC**.** During bulk electrolysis of DDC at 0.9 V vs. Ag which is higher than the peak potential E_2 (E_2 = 0.675 V vs SCE), optical spectra shown in Figure 6 were obtained. Before bulk electrolysis (spectrum (a) in Figure 6), the spectrum showed

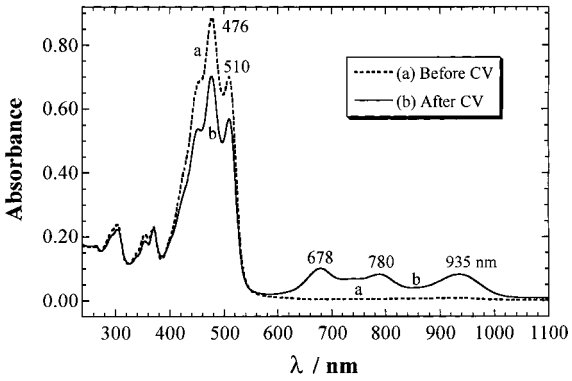

Figure 7. UV−visible absorption spectra for 0.01 mM DDC in a 0.05 M TBAHFP/CH_2Cl_2 solution: (a) before and (b) after running CV at scan rate of 10 mV/s in the potential window of −0.1 to 1.0 V.

only the absorption of neutral DDC at $\lambda = 476$ nm and two lower intensity peaks at 510 and 450 nm. After bulk electrolysis for 2 min, three additional peaks with maxima at 935, 780, and 678 nm appeared. The intensity of peaks 678 and 780 nm increased with time of electrolysis and the intensity of peak 476 nm decreased with the time. The intensity of peak 935 nm increased with time in the first 2 min and thereafter decreased with time of electrolysis.

Studies[14,21] have shown that absorption peaks of radical cations and dications of carotenoids are located in the region of 800 to 1500 nm. The 935 nm absorption band can be attributed to the radical cations of DDC because dications are not stable in the studied media, and they will easily form other products via reactions 4 and 5 as shown in Scheme 1. The 780 nm band is attributed to polymeric species formed during the electrochemical process. To further study the spectroelectrochemical behavior of DDC, UV−vis absorption spectra of DDC were also recorded at various applied potentials. On increasing the BE potential from 0.40 V to higher oxidation potentials (up to 1.0 V vs Ag), the absorption of neutral DDC at 476 nm continuously decreased with time, while the absorption of polymeric products at 780 nm steadily increased. However, the spectral absorption of the radical cations at 935 nm grew faster than the 678 and 780 nm peaks only during the first 2 min, and then decreased with time, which indicates that the radical cations of DDC are unstable and decay quite rapidly. We suspect that the 678 nm band may be due to the unidentified dimer of DDC, which could be formed by the reaction of radical cations with neutral DDC molecules. The same absorption bands were also observed after only one CV scan in the potential window of −0.1 to 1.0 V. As seen in Figure 7, three new absorption peaks occurred after running the CV. In other words, radical cations ($\lambda_{max} = 935$ nm) and polymeric products ($\lambda_{max} = 780$ nm) were formed during the anodic scan from −0.1 to 1.0 V vs. Ag. When scanning the potential back from 1.0 to −0.1 V (cathodic reduction process), the radical cations and polymeric products could not be electrochemically reduced.

Figure 8 depicts the simultaneous measurement of absorbance (at four main peak wavelengths) during potential scans in the range of −0.1 to 1.0 V vs Ag. During the anodic scan (Figure 8A), the decrease of the initially high absorbance of neutral DDC is observed at ca. 0.6 V, which is consistent with the anodic peak potentials as shown in Figure 1A ($E_1 = 0.600$ V and $E_2 = 0.675$ V vs SCE) corresponding to the formation of radical cations and dications of DDC. The concentration of neutral species continues to decrease by applying a potential

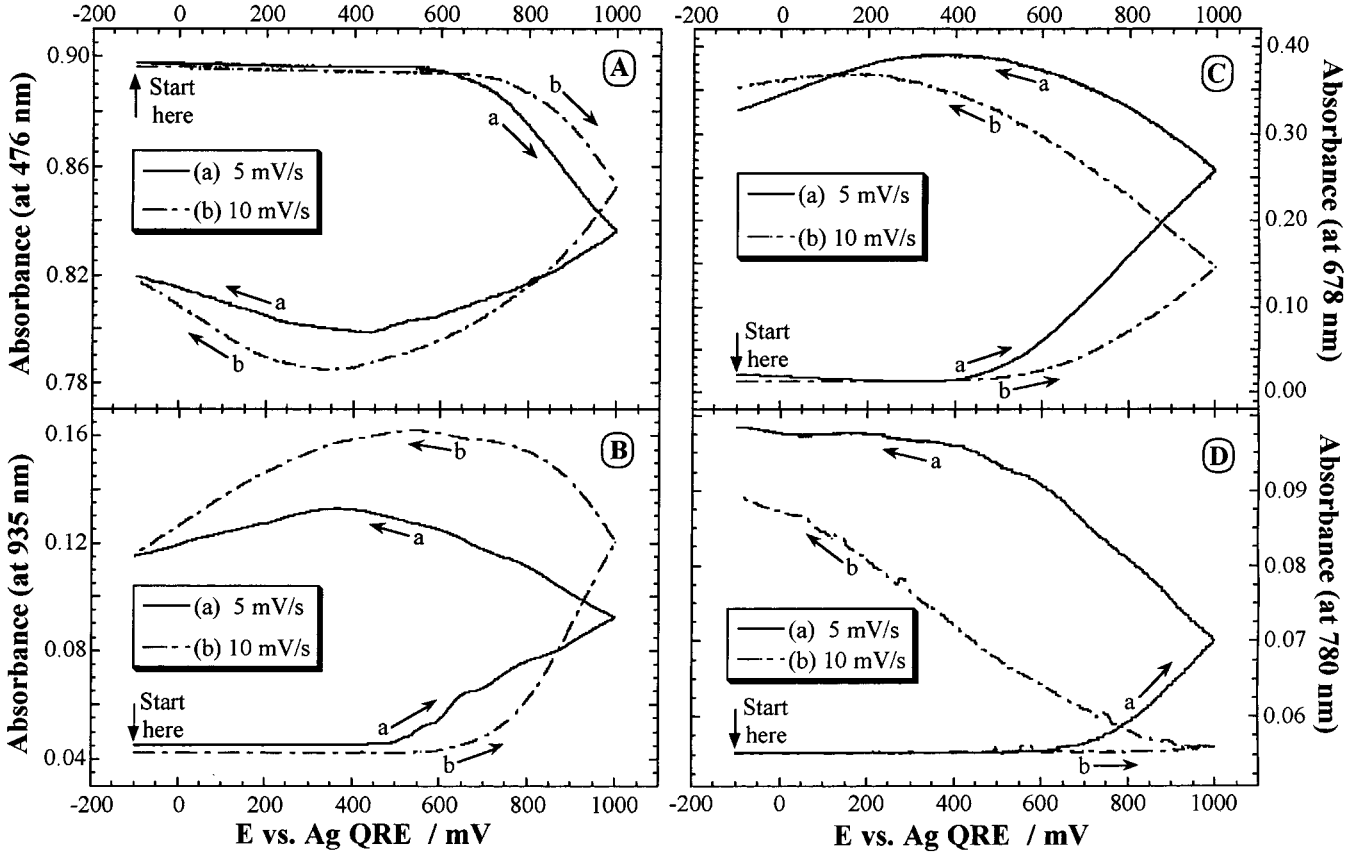

Figure 8. Simultaneous measurement of absorbance and applied potential of 0.01 mM DDC in 0.05 M TBAHFP/CH_2Cl_2 solutions during potential scan rate of (a) 5 and (b) 10 mV/s in the potential window −100 to 1000 mV. Absorbance was recorded at (A) 476, (B) 935, (C) 678, and (D) 780 nm.

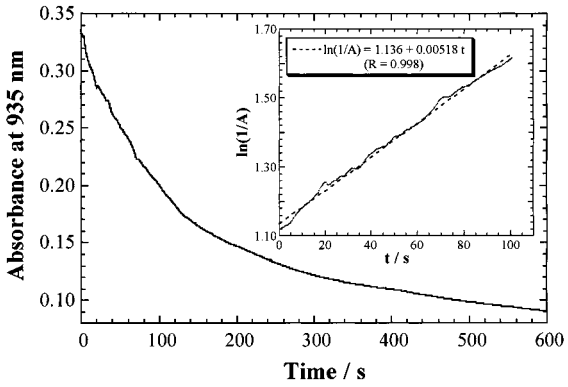

Figure 9. Time dependence of absorbance for radical cations of DDC at 935 nm. Decay rate measurement was conducted in 0.01 mM DDC−0.05 M TBAHFP/CH_2Cl_2 after bulk electrolysis for 2 min. Insert is the corresponding plot of the logarithms of the reciprocal of absorbance [ln(1/A)] against time (*t*).

that is higher than 0.6 V. The reaction products can be reduced only partly to the original neutral DDC as indicated by the increase of absorbance during the cathodic scan.

As deduced from Figure 8B,C, the potentials, at which the products started to be generated during the anodic scan, are as follows: 0.45 V for the radical cations (λ_{max} = 935 nm), 0.45 V for unidentified dimer products (λ_{max} = 678 nm), and 0.6 V vs Ag for polymeric products (λ_{max} = 780 nm). Polymeric products can only be formed at higher potential than the radical cations. The above results are reasonable since the polymeric species are formed[7] only after generation of the dications of DDC while applying a potential more positive than 0.675 V ($E_{2)}$ vs. SCE.

Kinetic Analysis. To examine the stability of the radical cations of DDC, the time dependence of its absorbance was measured (Figure 9). The decay rate of the reaction products can be considered as first-order kinetics. Thus, plots of the logarithms of the reciprocal of absorbance [ln(1/*A*)] against time (*t*) should yield a straight line, with the slope equal to *k*. The rate constant (*k*) and the half-lifetime ($t_{1/2}$) for the decay reaction of the radical cations of DDC were estimated as $k = (5.5 \pm 1.3) \times 10^{-3}$ (s^{-1}) and $t_{1/2} = 2.1 \pm 0.4$ (min). It is difficult to measure the stability of polymeric (λ_{max} = 780 nm) and unidentified (λ_{max} = 678 nm) products since (a) their decay rates appear to be zero-order kinetics as seen from the time dependence of absorbance and (b) their initial concentrations are not available. On the other hand, it can be seen from Figure 6 that the polymeric and unidentified products are much more stable than the radical cations.

Conclusions

In the present study, we found that long-chain alkanethiols, carboxylic acid-terminated, and hydroxyl-terminated SAMs have a profound barrier effect on the reaction of 7,7′-diapo-(7*E*,7′*Z*)-diphenylcarotene (DDC), but 4-MP SAMs exert only a very small barrier. The electron transfer is suppressed to about 60% by a long-chain *n*-alkanethiol-modified Au electrode. With increasing chain length of alkanethiol molecules, a stronger barrier effect for the adsorption of polymeric products is observed. DDC and its reaction products, including the radical cations and polymeric products, were also studied by using simultaneous optical and electrochemical techniques.

Acknowledgment. We thank Dr. Elli Hand for synthesizing 7,7′-diapo-(7*E*,7′*Z*)-diphenylcarotene as well as helpful discussions. This work was supported by the Division of Chemical Sciences, Office of Basic Energy Sciences of the U.S. Department of Energy under Grant DE-FG02-86-ER13465.

References and Notes

(1) (a) Ulman, A. *Chem. Rev.* **1996**, *96*, 1533−1554. (b) Mandler, D.; Turyan, I. *Electrolysis* **1996**, *8*, 207−213.

(2) (a) Ulman, A. *Introduction to Thin Organic Films: From Langmuir−Blodgett to Self-Assembly*; Academic Press: Boston, MA, 1991. (b) Kang, J.; Rowntree, P. A. *Langmuir* **1996**, *12*, 2813−2819.

(3) (a) Cooper, T. M.; Campbell, A. L.; Crane, R. M. *Langmuir* **1995**, *11*, 2713−2718. (b) Jordan, C. E.; Corn, R. M. *Anal. Chem.* **1997**, *69*, 1449−1456.

(4) Liu, D.; Gao, G.; Kispert, L. D. *50th Southeast Regional Meeting of the American Chemical Society*, Research Triangle Park, NC, 1998; p 115.

(5) (a) Gust, D.; Moore, T. A.; Moore, A. L.; Lee, S. J.; Bittersmann, E.; Luttrull, D. K.; Rehms, A. A.; DeGraziano, J. M.; Ma, X. C.; Gao, F.; Belford, R. E.; Trier, T. T. *Science* **1990**, *248*, 199−201. (b) Gust, D.; Moore, T. A.; Moore, A. L.; Makings, L. R.; Seely, G. R.; Ma, X.; Trier, T. T.; Gao, F. *J. Am. Chem. Soc.* **1988**, *110*, 7567−7569.

(6) Gao, G.; Jeevarajan, A. S.; Kispert, L. D. *J. Electroanal. Chem.* **1996**, *411*, 51−56.

(7) Gao, G.; Wurm, D. B.; Kim, Y.-T.; Kispert, L. D. *J. Phys. Chem. B* **1997**, *101*, 2038−2045.

(8) Liu, D.; Kispert, L. D. In *Recent Research Developments in Electrochemistry, Part II*; Pandalai, S. G., Ed.; Transworld Research Network: Trivandrum, India**,** 1999; Vol. 2, pp 139−157.

(9) Mairanovsky, V. G.; Engovatov, A. A.; Ioffe, N. T.; Samokhvalov, G. I. *J. Electroanal. Chem.* **1975**, *66*, 123−137.

(10) Jeevarajan, A. S.; Khaled, M.; Kispert, L. D. *J. Phys. Chem.* **1994**, *98*, 7777−7781.

(11) Jeevarajan, J. A.; Kispert, L. D. *J. Electroanal. Chem.* **1996**, *411*, 57−66.

(12) Hand, E. S.; Belmore, K. A.; Kispert, L. D. *Helv. Chim. Acta* **1993**, *76*, 1939−1948.

(13) Grant, J. L.; Kramer, V. J.; Ding, R.; Kispert, L. D. *J. Am. Chem. Soc.* **1988**, *110*, 2151−2157.

(14) Jeevarajan, A. S.; Kispert, L. D.; Wu, X. *Chem. Phys. Lett.* **1994**, *219*, 427−432.

(15) Bard, A. J.; Abruna, H. D.; Chidsey, C. E.; Faulkner, L. R.; Feldberg, S. W.; Itaya, K.; Majda, M.; Melroy, O.; Murray, R. W.; Porter, M. D.; Soriaga, M. P.; White, H. S. *J. Phys. Chem.* **1993**, *97*, 7147−7173.

(16) Finklea, H. O. In *Electroanalytical Chemistry*; Bard, A. J., Rubinstein, I., Eds.; Marcel Dekker: New York, 1996; Vol. 19, pp 109−335.

(17) (a) Zamborini, F. P.; Crooks, R. M. *Langmuir* **1998**, *14*, 3279−3286. (b) Yan, J.; Dong, S. *J. Electroanal. Chem.* **1997**, *440*, 229−238. (c) French, M.; Creager, S. E. *Langmuir* **1998**, *14*, 2129−2133.

(18) (a) Gao, Z.; Siow, K. S. *Electrochim. Acta* **1997**, *42*, 315−321. (b) Yang, D.; Zi, M.; Chen, B.; Gao, Z. *J. Electroanal. Chem.* **1999**, *470*, 114−119. (c) Che, G.; Li, Z.; Zhang, H.; Cabrera, C. R. *J. Electroanal. Chem.* **1998**, *453*, 9−17.

(19) Jenning, G. K.; Munro, J. C.; Young, T.-H.; Laibinis, P. E. *Langmuir* **1998**, *14*, 6130−6139.

(20) Britton, G. In *Carotenoids, Vol. 1B: Spectroscopy*; Britton, G., Liaaen-Jensen, S., Pfander, H., Eds.; Birkhäuser Verlag: Basel, 1995; p 57.

(21) Bensasson, R. V.; Land, E. J.; Truscott, T. G. *Flash Photolysis and Pulse Radiolysis*; Pergamon: Oxford, 1983.